

## Antiphase boundary-like structure in $\alpha''$ martensite of TC21 titanium alloy

XU Yan-fei<sup>1</sup>, LIU Hui-qun<sup>1,2</sup>, YI Dan-qing<sup>1,2</sup>, ZHU Zhi-shou<sup>3</sup>, ZHENG Feng<sup>1,2</sup>

1. School of Materials Science and Engineering, Central South University, Changsha 410083, China;

2. Key Laboratory of Nonferrous Metal Materials Sciences and Engineering, Ministry of Education, Central South University, Changsha 410083, China;

3. Beijing Institute of Aeronautical Materials, Beijing 100095, China

Received 10 February 2012; accepted 8 May 2012

**Abstract:** The morphology and formation mechanism of the substructure of martensite in TC21 alloy was investigated by XRD and TEM. The results showed that the martensitic transformation from  $\beta$  to  $\alpha''$  occurs upon quenching after solution treatment between 960–1000 °C. The antiphase boundary (APB)-like structure was observed clearly in the  $\alpha''$  martensite plates. The APB-like contrasts exist along the (001) and (020) planes of  $\alpha''$  martensite. This APB-like structure of  $\alpha''$  martensite was identified as a kind of stacking fault with an APB-like morphology induced by martensitic transformation and not by order/disorder transition. During martensitic transformation, martensitic domains nucleate and grow, eventually encounter each other, resulting in the formation of the APB-like contrast.

**Key words:** titanium alloy; martensitic transformation; antiphase boundary (APB); crystal structure

### 1 Introduction

Due to their excellent properties such as high specific strength, low density and high corrosion resistance, titanium alloys have been widely used in aerospace industry for several decades [1,2]. The increasing demand of fracture toughness at higher temperatures has prompted the development of novel Ti-based materials based on the design of damage tolerance with respect to strength. TC21 alloy is a new alpha-beta high strength and damage tolerance titanium alloy developed by Northwest Institute for Nonferrous Metal Research of China [3,4]. TC21 alloy was reported to have specific strength of 1050–1200 MPa and fracture toughness of  $\sim 72$  MPa·m<sup>1/2</sup> and was considered a potential structural material for aircraft applications [3].

Of course, structural stability is one of major concerns regarding its potential applications. In last decade, the research efforts have mainly been focused on the mechanical properties and deformation behavior of TC21 alloy [3–10]. But few works have been done in the field of microstructure and phase transformation. WANG et al [7] reported that orthorhombic  $\alpha''$  martensite was formed in TC21 alloy after solution treatment above

840 °C, but they did not focus on the substructure of  $\alpha''$  martensite. The substructure such as twins, dislocations or stacking faults have been found in  $\alpha''$  martensite of some other titanium alloys [11–13], but the substructure of martensite in TC21 alloy is still unclear. The purpose of this work is to clarify the morphology and formation mechanism of the substructure of martensite in TC21 alloy.

### 2 Experimental

TC21 alloy used in this study was provided by Western Superconducting Technologies Co., Ltd., China, in a hot forging condition. The normal composition of the alloy was Ti–6Al–3Mo–2Sn–2Nb–2Zr–1Cr (mass fraction, %). The chemical composition of the alloy analyzed by inductive coupled plasma–atomic emission spectrometry (ICP–AES) is listed in Table 1. The  $(\alpha+\beta)/\beta$  transus temperature ( $T_\beta$ ) of as-received TC21 alloy is 960 °C. As-received TC21 bars were cut into many small pieces (5 mm×10 mm×10 mm) and encapsulated in quartz tubes filled with Ar atmosphere. Then the specimens were solution treated between 960 °C and 1000 °C for 25 min at an interval of 10 °C, followed by water quenching. After quenching, the surface layers of

**Table 1** Chemical composition of TC21 alloy (mass fraction, %)

Al	Mo	Nb	Zr	Sn	Cr	Ti
6.97	2.75	1.83	2.04	1.69	1.47	Balance

the specimens were mechanically removed. Phase constitution and microstructures were investigated by X-ray diffraction (XRD), conventional transmission electron microscopy (CTEM) and high-resolution transmission electron microscopy (HRTEM). The XRD analysis was carried out on a Rigaku D/Max 2500 diffractometer with Cu  $K_{\alpha}$  radiation and graphite monochromator operated at 40 kV and 250 mA at a scanning speed of 1 ( $^{\circ}$ )/min. The samples for transmission electron microscopy (TEM) were mechanically ground and ion milled prior to examination. CTEM and HRTEM observations were conducted on FEI Tecnai G<sup>2</sup> 20 and FEI Tecnai G<sup>2</sup> F20 S-TWIN transmission electron microscopes, respectively, which were operated at 200 kV. Fast Fourier transformation (FFT) was carried out using the Digital Micrograph package.

### 3 Results and discussion

#### 3.1 Crystal structure of $\alpha''$ martensite

Figure 1 shows the XRD patterns of TC21 alloy as-received and after solution treatment at temperatures of 960  $^{\circ}$ C and 1000  $^{\circ}$ C. It is obvious that the peaks of  $\alpha$  and  $\beta$  phases are confirmed for as-received TC21 alloy. After solution treatment at 960  $^{\circ}$ C and 1000  $^{\circ}$ C, the peaks of orthorhombic  $\alpha''$  martensite and weak peak of  $\beta$  phase were observed whereas the peaks of  $\alpha$  phase disappeared. It suggests that the phase transformations of  $\alpha + \beta \rightarrow \beta$  and  $\beta \rightarrow \alpha''$  occurred after solution treatment between 960  $^{\circ}$ C and 1000  $^{\circ}$ C. This result is consistent with the previous report [7] that  $\beta$  phase transformed to

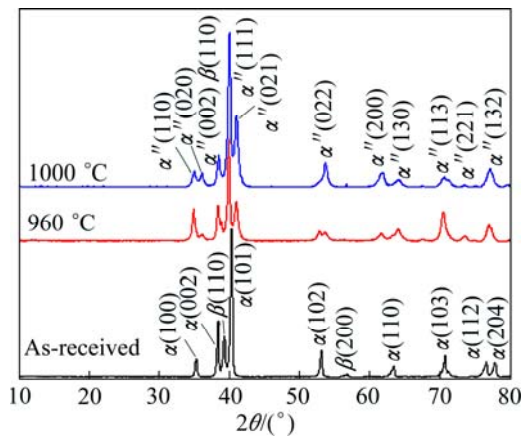


**Fig. 1** XRD patterns of as-received and solution treated TC21 alloy at 1000  $^{\circ}$ C and 960  $^{\circ}$ C respectively

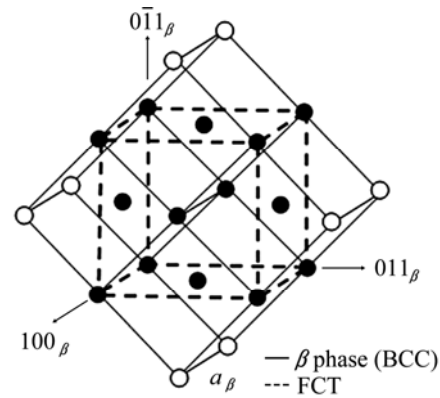
$\alpha''$  martensite in TC21 alloy after solution treatment above 840  $^{\circ}$ C. According to the XRD patterns, the lattice parameters of  $\alpha''$  martensite were determined as follows:  $a=3.002$   $\text{\AA}$ ,  $b=4.975$   $\text{\AA}$  and  $c=4.684$   $\text{\AA}$  after 960  $^{\circ}$ C treatment;  $a=2.996$   $\text{\AA}$ ,  $b=4.978$   $\text{\AA}$  and  $c=4.689$   $\text{\AA}$  after 1000  $^{\circ}$ C treatment.

The structure of  $\alpha''$  martensite is believed to be C-centred orthorhombic crystal structure with a  $Cmcm$  space group, derived from a body-centered cubic (BCC) lattice ( $\beta$  phase) [14]. Figure 2 shows a schematic illustration of lattice correspondence between BCC  $\beta$  phase and orthorhombic  $\alpha''$  martensite [13]. The parent BCC  $\beta$  phase is marked with solid lines and its lattice parameter is  $a_{\beta}$ . The face-centered tetragonal (FCT) cell (marked with thick-dashes) is further distorted to form an orthorhombic cell with lattice parameters of  $a$ ,  $b$  and  $c$ , where  $a < c < b$ . The atoms for  $\alpha''$  martensite locate at (0, 0, 0), (1/2, 1/2, 0), (0, 1-2y, 1/2) and (0, 1/2-2y, 1/2) positions. The lattice correspondence between  $\beta$  phase and  $\alpha''$  martensite can be expressed as follows:

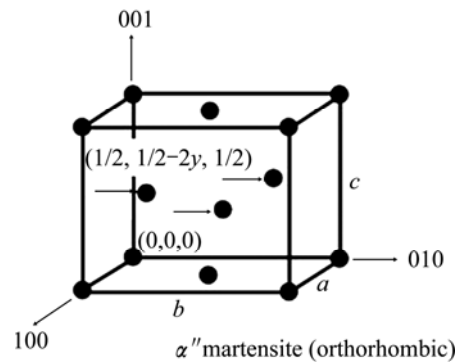
$$[100]_{\beta} - [100]_{\alpha''}, [010]_{\beta} - \frac{1}{2}[01\bar{1}]_{\alpha''}, [001]_{\beta} - \frac{1}{2}[011]_{\alpha''}$$

or

$$[100]_{\alpha''} - [100]_{\beta}, [010]_{\alpha''} - \frac{1}{2}[011]_{\beta}, [001]_{\alpha''} - \frac{1}{2}[0\bar{1}\bar{1}]_{\beta}$$



(a)



(b)

**Fig. 2** Schematic illustration showing lattice correspondence between  $\beta$  phase and  $\alpha''$  martensite [13]

### 3.2 APB-like fault in $\alpha''$ martensite

Figure 3 exhibits the bright-field images and corresponding selected area electron diffraction (SAED) pattern of TC21 alloy after solution treatment at 970 °C. The martensite plates with different orientations are observed in Fig. 3(a), which is consistent with the result of XRD (Fig. 1). Figure 3(b) shows a high-magnification micrograph where many line and curved contrasts are seen clearly in martensite plates. Figure 3(c) shows the details of these line and curved contrasts. Figure 3(d) shows the corresponding SAED pattern taken from Fig. 3(c) along  $[100]_{\alpha''}$  zone axis, which confirms that the martensite plate is orthorhombic  $\alpha''$  martensite. As is apparent from the SAED pattern, the line contrasts along the (001) and (020) planes of  $\alpha''$  martensite are seen clearly in Fig. 3(c). In addition to this kind of ledge-and-step structure on the  $b$ - $c$  plane, some angular closed looped contrasts are also observed in this martensite plate. Other than that at 970 °C, the contrasts within  $\alpha''$  martensite plates were observed in all samples after solution treatment between 960–1000 °C.

These line and curved contrasts have a morphology

similar to the antiphase boundary (APB) of ordered alloy which was previously observed in other titanium alloys [11,15]. It has been widely recognized that  $\pi$  contrast of the APB induced by order/disorder transformation can be observed using superlattice reflections for the ordered structure, whereas no contrast is observed using fundamental reflections [16,17]. These contrasts in the present study are visible when  $g=001_{\alpha''}$  superlattice reflection is used in the  $[100]_{\alpha''}$  zone. In order to determine whether these contrasts are APBs or APB-like contrasts, it is necessary to observe these contrasts using fundamental reflection. Figure 4 shows the dark-field images taken by using  $g=020_{\alpha''}$  fundamental reflection in  $[100]_{\alpha''}$  zone for the alloy after solution treatment at 960 and 990 °C, respectively. The contrasts can be clearly observed when the  $020_{\alpha''}$  fundamental reflection is used, as shown in Figs. 4(a) and (b). These facts indicate that the contrast does not correspond to a  $\pi$  contrast of APB but an APB-like structure.

### 3.3 Formation mechanism of APB-like contrast

The APB-like structure has also been found in

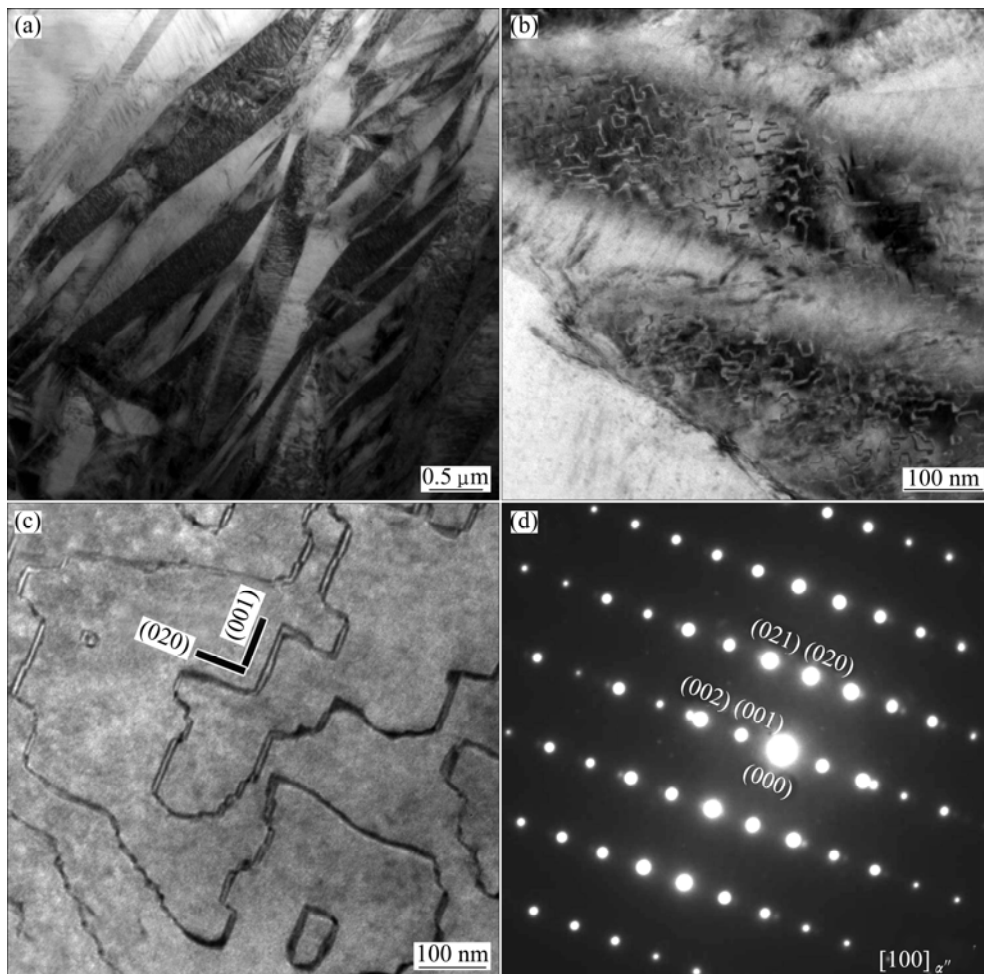


**Fig. 3** Bright-field images of TC21 alloy solution treated at 970 °C: (a)  $\alpha''$  martensite plates; (b) APB-like structure in  $\alpha''$  martensite plates; (c) High magnification of APB-like structure in a large  $\alpha''$  plate; (d) SAED pattern taken from (c) along  $[100]_{\alpha''}$  zone axis

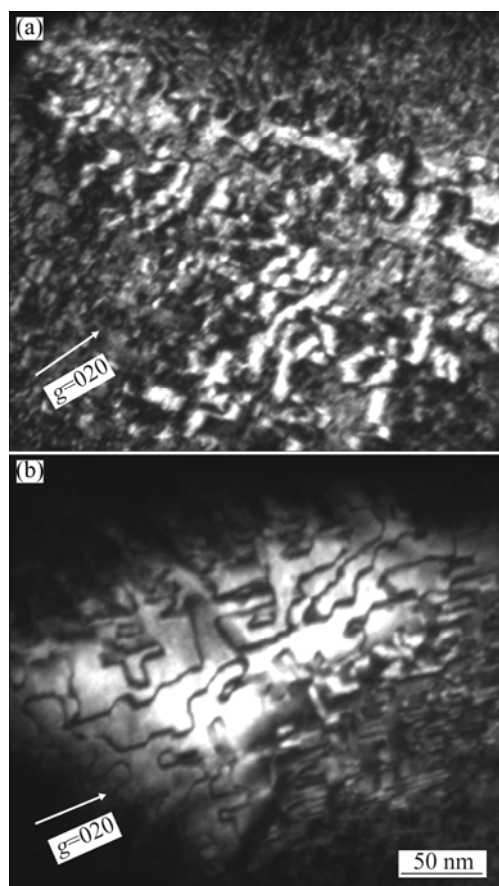


**Fig. 4** Dark-field images showing APB-like contrast with  $g=020_{\alpha''}$  in  $[100]_{\alpha''}$  zone of TC21 alloy solution treated at 960 °C (a) and 990 °C (b)

hexagonal  $\alpha'$  martensite of Ti–Al–Mo–Zr–Si [18], B19 martensite of Ti–Pd [17], B19' martensite of Ti–Ni [19] and  $\alpha''$  martensite of Ti–V–Al [11], Ti–Nb [12] and Ti–Nb–Al [13] alloys. PAK et al [11] and AHMED and RACK [12] assumed that  $\alpha''$  martensite has an ordered structure to explain the APB-like structure. Recently, INAMURA et al [13] investigated the APB-like structure in  $\alpha''$  martensite by dark-field TEM using different reflections and proposed that the APB-like structure is a stacking fault and not related to ordering. However, the APB-like structure in  $\alpha''$  martensite has not been observed at the atomic level.

In order to analyze the APB-like contrast at the atomic level, HRTEM observation was carried out along  $[100]_{\alpha''}$  zone axis for the alloy after solution treatment at 970 °C, as shown in Fig. 5. An APB-like contrast is clearly observed in Fig. 5(a), and the corresponding FFT pattern (inset) shows both the (100) and (020) lattice planes from  $\alpha''$  martensite. Figure 5(b) shows the corresponding inverse FFT image of the area of the frame in Fig. 5(a). The atomic shifts of the  $(001)_{\alpha''}$  plane can be identified by the shift of bright spots, as marked by the white arrows. The APB-like contrast is nearly

parallel to the (020) plane of  $\alpha''$  martensite, as indicated by the dark arrows. The APB is a boundary where no atomic shift is present when atoms of different types in ordered alloys are replaced by atoms of the same type [19]. In the case of a stacking fault, the atomic shift exists at the interface irrespective of the elements. Thus, the observations of CTEM and HRTEM demonstrate that the APB-like structure of  $\alpha''$  martensite is a kind of stacking fault with an APB-like morphology induced by displacive transformation.

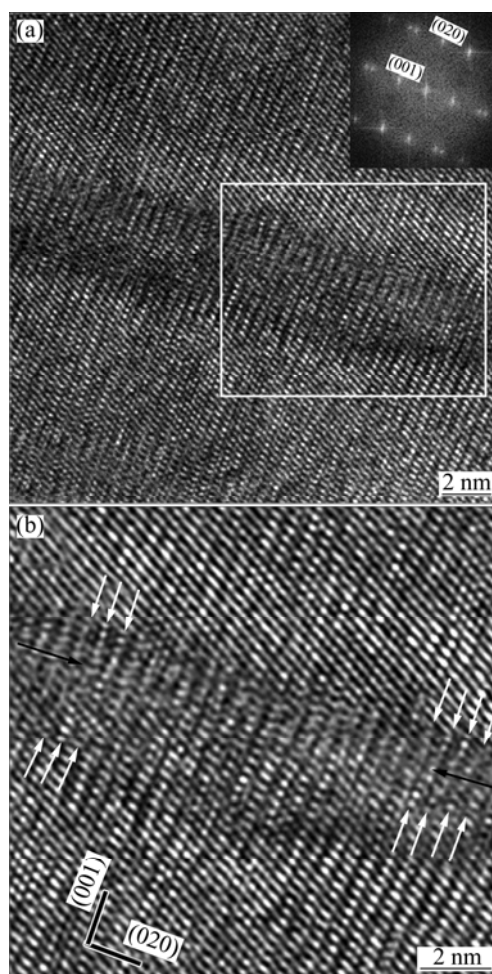


**Fig. 5** HRTEM image with corresponding FFT pattern (inset) of APB-like structure along  $[100]_{\alpha''}$  zone axis of TC21 alloy after solution treatment at 970 °C (a) and inverse FFT image of area of frame in Fig. 5(a) (b)

The displacement vector  $\mathbf{R}$  of the APB-like fault,  $\mathbf{R}=[R_x R_y R_z]$ , can be evaluated by  $\mathbf{g}\cdot\mathbf{R}$  analysis using the axial dark-field mode at the exact Bragg position, where  $\mathbf{g}$  is a reciprocal lattice vector indicating a diffracting plane. The relationship between the phase angle  $\alpha$  of the diffracted wave and  $\mathbf{R}$  is given by  $\alpha=2\pi\mathbf{g}\cdot\mathbf{R}$  [16]. When the value of  $\mathbf{g}\cdot\mathbf{R}$  is an integer, the contrast of the fault is theoretically invisible. The displacement vector  $\mathbf{R}$  of the APB-like fault is equal to the displacement caused by

atomic shuffling during the martensitic transformation [17,19]. The values of  $\mathbf{R}$  were reported to be  $[1/3 \ 0 \ -1/2]$  for B19 martensite of Ti–Pd [17] and  $[-0.1648 \ 1/2 \ 0.4328]$  for B19' martensite of Ti–Ni [19]. For  $\alpha''$  martensite, the  $\mathbf{R}$  of the APB-like fault was determined by  $\mathbf{g}\cdot\mathbf{R}$  analysis to be  $[R_x \ R_y \ 1/2]$ , where  $2R_x+4R_y$  is almost an integer and  $R_x+R_y$  is almost a half-integer [13]. In the present study, the results of  $\mathbf{g}\cdot\mathbf{R}$  analysis are in good agreement with the previous report [13].

Combining with the analyses of CTEM and HRTEM, it is concluded that the APB-like contrast is induced by the martensitic transformation. The APB-like contrast along the (001) and (020) planes of  $\alpha''$  martensite was observed obviously, as shown in Fig. 3(c) and Fig. 5. And then, a mechanism for the formation of the APB-like contrast of  $\alpha''$  martensite can be proposed on the basis of these observations. Figure 6 shows a schematic illustration of a mechanism for the formation of the APB-like contrast. During the martensitic transformation from  $\beta$  (BCC) to  $\alpha''$  martensite (orthorhombic), martensitic domains nucleate at various sites within a variant. Two neighboring domains grow and eventually encounter each other, resulting in the formation of the APB-like interface. In other words, the impingement of such domains produces the APB-like contrast.

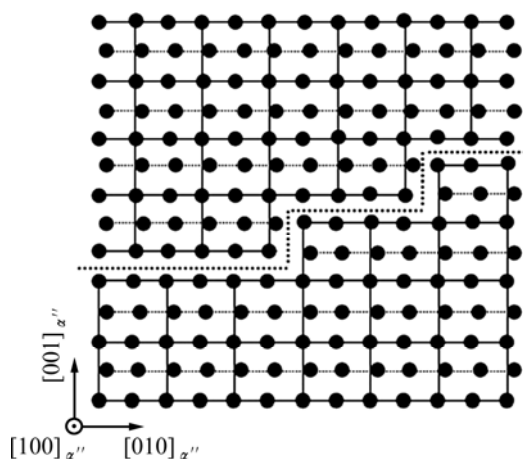


Fig. 6 Schematic illustration showing formation mechanism of APB-like contrast in  $\alpha''$  martensite

## 4 Conclusions

The morphology and formation mechanism of the APB-like fault in  $\alpha''$  martensite of TC21 alloy were investigated.  $\beta \rightarrow \alpha''$  martensitic transformation occurred upon quenching after solution treatment at 960–1000 °C. The APB-like structure is formed in  $\alpha''$  martensite plates during martensitic transformation. The APB-like contrast lies parallel to the (001) and (020) planes of  $\alpha''$  martensite. The APB-like structure of  $\alpha''$  martensite is defined as a kind of stacking fault with an APB-like

morphology induced by displacement transformation and not by order/disorder transition. The APB-like contrast is developed by impingement of different nucleated martensitic domains during martensitic transformation.

## References

- [1] BOYER R R. An overview on the use of titanium in the aerospace industry [J]. Materials Science and Engineering A, 1996, 213: 103–114.
- [2] WILLIAMS J C, STARKE E A Jr. Progress in structural materials for aerospace systems [J]. Acta Materialia, 2003, 51: 5775–5799.
- [3] ZHAO Yong-qing, QU Heng-lei, FENG Liang, YANG Hai-ying, LI Hui, ZHANG Ying-nan, GUO Hong-chao, HUANG Ding-kun. Research on high strength, high toughness and high damage-tolerant titanium alloy—TC21 [J]. Titanium Industry Progress, 2004, 21(1): 22–24. (in Chinese)
- [4] ZHANG Ying-nan, ZHAO Yong-qing, QU Heng-lei, LI Hui, FENG Liang, GUO Hong-chao, HUANG Ding-kun. Effect of heat treatment on microstructure and tensile properties of TC21 alloy [J]. Chinese Journal of Rare Metals, 2004, 28(1): 34–38. (in Chinese)
- [5] CHEN Jun, ZHAO Yong-qing, ZENG Wei-dong. Effect of microstructure on impact toughness of TC21 alloy [J]. Transactions of Nonferrous Metals Society of China, 2007, 17(s1): s93–s98.
- [6] FEI Y, ZHOU L, QU H, ZHAO Y, HUANG C. The phase and microstructure of TC21 alloy [J]. Materials Science and Engineering A, 2008, 494: 166–172.
- [7] WANG Y H, KOU H, CHANG H, ZHU Z S, ZHANG F S, LI J, ZHOU L. Influence of solution temperature on phase transformation of TC21 alloy [J]. Materials Science and Engineering A, 2009, 508: 76–82.
- [8] GONG X, WANG Y, XIA Y, GE P, ZHAO Y. Experimental studies on the dynamic tensile behavior of Ti–6Al–2Sn–2Zr–3Mo–1Cr–2Nb–Si alloy with Widmanstatten microstructure at elevated temperatures [J]. Materials Science and Engineering A, 2009, 523: 53–59.
- [9] ZHAO Yan-lei, LI Bo-long, ZHU Zhi-shou, NIE Zuo-ren. Influence of high temperature deformation parameters on microstructure and properties of TC21 titanium alloy [J]. The Chinese Journal of Nonferrous Metals, 2010, 20(s1): s132–s137. (in Chinese)
- [10] ZHU Y C, ZENG W D, LIU J L, ZHAO Y Q, ZHOU Y G, YU H Q. Effect of processing parameters on the hot deformation behavior of as-cast TC21 titanium alloy [J]. Materials Design, 2012, 33: 264–272.
- [11] PAK J S L, LEI C Y, WAYMAN C M. Atomic ordering in Ti–V–Al shape memory alloys [J]. Materials Science and Engineering A, 1991, 132: 237–244.
- [12] AHMED T, RACK H J. Martensitic transformations in Ti–(16–26 at %) Nb alloys [J]. Journal of Materials Science, 1996, 31: 4267–4276.
- [13] INAMURA T, HOSODA H, KIM H Y, MIYAZAKI S. Antiphase boundary-like stacking fault in  $\alpha''$ -martensite of disordered crystal structure in  $\beta$ -titanium shape memory alloy [J]. Philosophical Magazine, 2010, 90: 3475–3498.
- [14] BROWN A R G, CLARK D, EASTABROOK J, JEPSON K S. The titanium–niobium system [J]. Nature, 1964, 201: 914–915.
- [15] MATSUDA M, HARA T, OKUNISHI E, NISHIDA M. High-angle annular dark field scanning transmission electron microscopy of the antiphase boundary in a rapidly solidified B2 type TiPd compound [J]. Philosophical Magazine Letters, 2007, 87: 59–64.
- [16] THOMAS G, WASHBURN J. Electron microscopy and strength of crystals [M]. New York: Interscience, 1963: 333–440.
- [17] MATSUDA M, HARA T, NISHIDA M. Crystallography and morphology of antiphase boundary-like structure induced by

- martensitic transformation in Ti–Pd shape memory alloy [J]. Materials Transactions, 2008, 49: 461–465.
- [18] BANERJEE D, MURALEEDHARAN K, STRUDEL J L. Substructure in titanium alloy martensite [J]. Philosophical Magazine A, 1998, 77: 299–323.
- [19] MATSUDA M, KURAMOTO K, MORIZONO Y, TSUREKAWA S, OKUNISHI E, HARA T, NISHIDA M. Transmission electron microscopy of antiphase boundary-like structure of B19' martensite in Ti–Ni shape memory alloy [J]. Acta Materialia, 2011, 59: 133–140.

## TC21 钛合金 $\alpha''$ 马氏体中的反相畴界状结构

许艳飞<sup>1</sup>, 刘会群<sup>1,2</sup>, 易丹青<sup>1,2</sup>, 朱知寿<sup>3</sup>, 郑 峰<sup>1,2</sup>

1. 中南大学 材料科学与工程学院, 长沙 410083;
2. 中南大学 有色金属材料科学与工程教育部重点实验室, 长沙 410083;
3. 北京航空材料研究院, 北京 100095

**摘 要:** 采用 X 射线衍射(XRD)和透射电子显微镜(TEM), 研究 TC21 钛合金马氏体中亚结构的形貌和形成机理。结果显示, 在 960~1000 °C 温度范围内, TC21 合金进行固溶淬火处理后会发生  $\beta \rightarrow \alpha''$  马氏体相变。在板条状  $\alpha''$  马氏体内部发现有反相畴界状结构, 并且该结构平行于  $\alpha''$  马氏体的(001)和(020)面。该结构被确定为马氏体相变过程中诱导产生的一种堆垛层错, 它具有反相畴界的形貌特征, 但并不是有序/无序相变过程中产生的反相畴界。在马氏体相变过程中, 马氏体畴形核并且长大, 畴与畴之间相互碰撞, 最终导致反相畴界状结构的产生。

**关键词:** 钛合金; 马氏体相变; 反相畴界; 晶体结构

(Edited by YUAN Sai-qian)